

Quantum CISC Compilation by Optimal Control and Scalable Assembly of Complex Instruction Sets beyond Two-Qubit Gates

T. Schulte-Herbrüggen,* A. Spörl, and S.J. Glaser

Department of Chemistry, Technical University Munich, D-85747 Garching, Germany

(Dated: 14th February 2019)

We present a quantum CISC compiler and show how to assemble complex instruction sets in a scalable way. Enlarging the toolbox of universal gates by optimised complex multi-qubit instruction sets thus paves the way to fight decoherence for realistic settings.

Compiling a quantum module into the machine code for steering a concrete quantum hardware device lends itself to be tackled by means of optimal quantum control. To this end, there are two opposite approaches: (i) one may use a decomposition into the restricted instruction set (RISC) of universal one- and two-qubit gates, which in turn have prefabricated translations into the machine code or (ii) one may prefer to generate the entire target module directly by a complex instruction set (CISC) of available controls. Here we advocate direct compilation up to the limit of system size a classical high-performance parallel computer cluster can reasonably handle. For going beyond these limits, i.e. for large systems we propose a combined way, namely (iii) to make recursive use of medium-sized building blocks generated by optimal control in the sense of a quantum CISC compiler.

The advantage of the method over standard RISC compilations into one- and two-qubit universal gates is explored on the parallel cluster HLRB-II (with a total LINPACK performance of 63.3 TFlops/s) for the quantum Fourier transform, the indirect SWAP gate as well as for multiply-controlled NOT gates. Implications for upper limits to time complexities are also derived.

PACS numbers: 03.67.-a, 03.67.Lx, 03.65.Yz, 03.67.Pp; 82.56.-b, 82.56.Jn, 82.56.Dj, 82.56.Fk

Introduction

Richard Feynman's seminal conjecture of using experimentally controllable quantum systems to perform computational tasks [1, 2] roots in reducing the complexity of the problem when moving from a classical setting to a quantum setting. The most prominent pioneering example being Shor's quantum algorithm of prime factorisation [3, 4] which is of polynomial complexity (BQP) on quantum devices instead of showing non-polynomial complexity on classical ones [5]. It is an example of a class of quantum algorithms [6, 7] that solve *hidden subgroup problems* in an efficient way [8], where in the Abelian case, the speed-up hinges on the quantum Fourier transform (QFT). Whereas the network complexity of the fast Fourier transform (FFT) for n classical bits is of order $O(n2^n)$ [9, 10], the QFT for n qubits shows a complexity of order $O(n^2)$. Moreover, Feynman's second observation that quantum systems may be used to efficiently predict the behaviour of other quantum systems has inaugurated a branch of research dedicated to Hamiltonian simulation [11, 12, 13, 14, 15, 16].

For implementing a quantum algorithm in an experimental setup, local operations and universal two-qubit quantum gates are required as a minimal set ensuring every unitary module can be realised [17]. More recently, it turned out that generic qubit and qudit pair interaction Hamiltonians suffice to complement local actions to universal controls [18, 19]. Common sets of quantum com-

putational instructions comprise (i) local operations such as the Hadamard gate, the phase gate and (ii) the entangling operations CNOT, controlled-phase gates, $\sqrt{\text{SWAP}}$, $i\text{SWAP}$ as well as (iii) the SWAP operation. The number of elementary gates required for implementing a quantum module then gives the network or gate complexity. However, gate complexity often translates into too coarse an estimate for the actual time required to implement a quantum module (see e.g. [20, 21, 22]), in particular, if the time scales of a specific experimental setting have to be matched. Instead, effort has been taken to give upper bounds on the actual time complexity [23], e.g., by way of numerical optimal control [24].

Interestingly, in terms of quantum control theory, the *existence of universal gates* is equivalent to the statement that the quantum system is *fully controllable* as has first been pointed out in Ref. [25]. This is, e.g., the case in systems of n spin- $\frac{1}{2}$ qubits that form Ising-type weak-coupling topologies described by arbitrary connected graphs [26, 27, 28]. Therefore the usual approach to quantum compilation in terms of local plus universal two-qubit operations [29, 30, 31, 32, 33] lends itself to be complemented by optimal-control based direct compilation into machine code: it may be seen as a technology-dependent optimiser in the sense of Ref. [32], however, tailored to deal with more complex instruction sets than the usual local plus two-qubit building blocks. Not only is it adapted to the specific experimental setting, it also allows for fighting decoherence by either being near timeoptimal or by exploiting decoherence-protected subspaces [34]. Devising quantum compilation methods for optimised realisations of given quantum algorithms by admissible controls is therefore an issue of

*Electronic address: tosh@ch.tum.de

considerable practical interest. Here it is the goal to show how quantum compilation can favourably be accomplished by optimal control: the building blocks for gate synthesis will be extended from the usual set of restricted local plus universal two-qubit gates to a larger toolbox of *scalable* multi-qubit gates tailored to yield high fidelity in short time given concrete experimental settings.

Quantum Compilation as an Optimal Control Task

As shown in Fig. 1, the quantum compilation task can be addressed following different principle guidelines: **(1)** by the standard decomposition into local operations and universal two-qubit gates, which by analogy to classical computation was termed *reduced instruction set* quantum computation (RISC) [35] or **(2)** by using direct compilation into one single *complex instruction set* (CISC) [35]. The existence of a such a single effective gate is guaranteed simply by the unitaries forming a group: a sequence of local plus universal gates is a product of unitaries and thus a single unitary itself.

As a consequence, CISC quantum compilation lends itself for resorting to numerical optimal control (on clusters of classical computers) for translating the unitary target module directly into the ‘machine code’ of evolutions of the quantum system under combinations of the drift Hamiltonian H_0 and experimentally available controls H_j .

In a number of studies on quantum systems up to 10 qubits, we have shown that direct compilation by gradient-assisted optimal control [24, 36, 37] allows for substantial speed-ups, e.g., by a factor of 5 for a CNOT and a factor of 13 for a Toffoli-gate on coupled Josephson qubits [37]. However, the direct approach naturally faces the limits of computing quantum systems on classical devices: upon parallelising our C++ code for high-performance clusters [38], we found that extending the quantum system by one qubit increases the CPU-time required for direct compilation into the quantum machine code of controls by grossly a factor of eight. So the classical complexity for optimal-control based quantum compilation is NP.

Therefore, here we advocate a third approach **(3)** that uses direct compilation into multi-qubit complex instruction sets up to the CPU-time limits of optimal quantum control on classical computers: these building blocks are designed such as to allow for recursive scalable quantum compilation in large quantum systems (i.e. those beyond classical computability). In particular, the complex instruction sets may be optimised such as to fight decoherence by being near time-optimal, or, moreover, they may be devised such as to fight the specific imperfections of an experimental setting.

Controllability

Before turning to optimal-control based CISC quantum compilation in more detail, it is important to ensure the quantum control system characterised by $\{H_0\} \cup \{H_j\}$ is in fact *fully controllable*.

Hamiltonian quantum dynamics following Schrödinger’s equation for the unitary image of a complete basis set of ‘state vectors’ representing a quantum gate

$$|\dot{\psi}(t)\rangle = -i(H_d + \sum_{j=1}^m u_j(t)H_j) |\psi(t)\rangle \quad (1)$$

$$\dot{U}(t) = -i(H_d + \sum_{j=1}^m u_j(t)H_j) U(t) \quad , \quad (2)$$

resembles the setting of a standard *bilinear control system* with state $X(t)$, drift A , controls B_j , and control amplitudes $u_j \in \mathbb{R}$ reading

$$\dot{X}(t) = (A + \sum_{j=1}^m u_j(t)B_j) X(t) \quad , \quad (3)$$

where $X(t) \in GL_N(\mathbb{C})$ and $A, B_j \in \text{Mat}_N(\mathbb{C})$. Clearly in the dynamics of closed quantum systems, the system Hamiltonian H_d is the drift term, whereas the H_j are the control Hamiltonians with $u_j(t)$ as control amplitudes. In systems of n qubits, $|\psi\rangle \in \mathbb{C}^{2^n}$, $U \in SU(2^n)$, and $iH_\nu \in \mathfrak{su}(2^n)$.

A system is *fully operator controllable*, if to every initial state ρ_0 the entire unitary orbit $\mathcal{O}_U(\rho_0) := \{U\rho_0U^\dagger \mid U \in SU(N)\}$ can be reached. With density operators being Hermitian this means any final state $\rho(t)$ can be reached from any initial state ρ_0 as long as both of them share the same spectrum of eigenvalues.

As established in [39], the bilinear system of Eqn. 2 is fully controllable if and only if the drift and controls are a generating set of $\mathfrak{su}(N)$ by way of the commutator, i.e., $(H_d, H_j \mid j = 1, 2, \dots, m)_{\text{Lie}} = \mathfrak{su}(N)$.

Example 1 Consider a system of n weakly coupled spin- $\frac{1}{2}$ qubits. Let $\sigma_x = \begin{pmatrix} 0 & 1 \\ 1 & 0 \end{pmatrix}$, $\sigma_y = \begin{pmatrix} 0 & -i \\ i & 0 \end{pmatrix}$, $\sigma_z = \begin{pmatrix} 1 & 0 \\ 0 & -1 \end{pmatrix}$ be the Pauli matrices. In n spins- $\frac{1}{2}$, a σ_{kx} for spin k is tacitly embedded as $\mathbf{1} \otimes \dots \otimes \mathbf{1} \otimes \sigma_x \otimes \mathbf{1} \otimes \dots \otimes \mathbf{1}$ where σ_x is at position k . The same holds for σ_{ky} , σ_{kz} , and in the weak coupling terms $\sigma_{kz}\sigma_{\ell z}$ with $1 \leq k < \ell \leq n$.

Now a system of n qubits is fully controllable [26], if e.g. the control Hamiltonians H_j comprise the Pauli matrices $\{\sigma_{kx}, \sigma_{ky} \mid k = 1, 2, \dots, n\}$ on every single qubit selectively and the drift Hamiltonian H_d encompasses the Ising pair interactions $\{J_{k\ell} (\sigma_{kz}\sigma_{\ell z})/2 \mid k < \ell = 2, \dots, n\}$, where the coupling topology of $J_{k\ell} \neq 0$ may take the form of any connected graph. This theorem has meanwhile been generalised to other coupling types [40, 41].

In view of the compilation task in quantum computation we get the following synopsis:

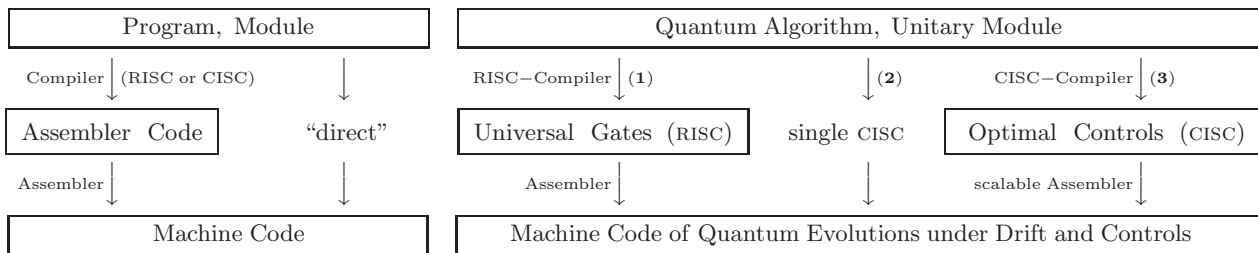


Figure 1: Compilation in classical computation (left) and quantum computation (right). Quantum machine code has to be time-optimal or protected against dissipation, otherwise decoherence wipes out the coherent superpositions. A quantum RISC-compiler (1) by universal gates leads to unnecessarily long machine code. Direct CISC-compilation into a single pulse sequence (2) exploits quantum control for a near time-optimal quantum machine code. Its classical complexity is NP, so direct compilation by numerical optimal control resorting to a classical computer is unfeasible for large quantum systems. The third way (3) promoted here pushes quantum CISC-compilation to the limits of classical supercomputer clusters and then assembles the multi-qubit complex instructions sets recursively into time-optimised or dissipation-protected quantum machine code.

Corollary 1 *The following are equivalent:*

- (1) *in a quantum system of n coupled spins- $\frac{1}{2}$, the drift H_d and the controls H_j form a generating set of $\mathfrak{su}(2^n)$;*
- (2) *the quantum system is operator controllable (in the sense of Ref. [42]);*
- (3) *every unitary transformation $U \in SU(2^n)$ can be realised by that system;*
- (4) *there is a set of universal quantum gates for the quantum system.*

Proof: The equivalence of (1) and (2) relies on the unitary group being a compact connected Lie group: compact connected Lie groups have no closed *subsemigroups* that are no groups themselves [39]. Moreover, in compact connected Lie groups the exponential mapping is surjective, hence (1) \Rightarrow (3). Assertions (3) and (4) just re-express the same fact in different terminology. ■

Scope and Organisation of the Paper

The purpose of this paper is to show that optimal control theory can be put to good use for devising multi-qubit building blocks designed for scalable quantum computing in realistic settings. Note these building blocks are no longer meant to be universal *in the practical sense* that any arbitrary quantum module should be built from them (plus local controls). Rather they provide specialised sets of complex instructions tailored for breaking down typical tasks in quantum computation with substantial speed gains compared to the standard compilation by decomposition into one-qubit and two-qubit gates. Thus a CISC quantum compiler translates into significant progress in fighting decoherence.

For demonstrating quantum CISC compilation and scalable assembly, in this paper we choose systems with linear

coupling topology, i.e., qubit chains coupled by nearest-neighbour Ising interactions. The paper is organised as follows: CISC quantum compilation by optimal control will be illustrated in three different, yet typical examples

- (1) the indirect $1, n$ -SWAP gate,
- (2) the quantum Fourier transform (QFT),
- (3) the generalisation of the CNOT and Toffoli gate to multiply-controlled NOT gates, C^n NOT.

For every instance of n -qubit systems, we analyse the effects of (i) sacrificing universality by going to special instruction sets tailored to the problem, (ii) extending pair interaction gates to effective multi-qubit interaction gates, and (iii) we compare the time gain by recursive m -qubit CISC-compilation ($m \leq n$) to the two limiting cases of the standard RISC-approach ($m = 2$) on one hand and the (extrapolated) time-complexity inferred from single-CISC compilation (with $m = n$).

Preliminaries

Time Standards

When comparing times to implement unitary target gates by the RISC *vs* the CISC approach, we will assume for simplicity that local unitary operations are ‘infinitely’ fast compared to the duration of the Ising coupling evolution so that the total gate time is solely determined by the coupling evolutions unless stated otherwise. Let us emphasise, however, this stipulation only concerns the time standards. The optimal-control assisted CISC-compilation methods presented here are in no way limited to fast local controls. In particular, also the assembler step of concatenating the CISC-building blocks is independent of the ratio of times for local operations *vs* coupling interactions.

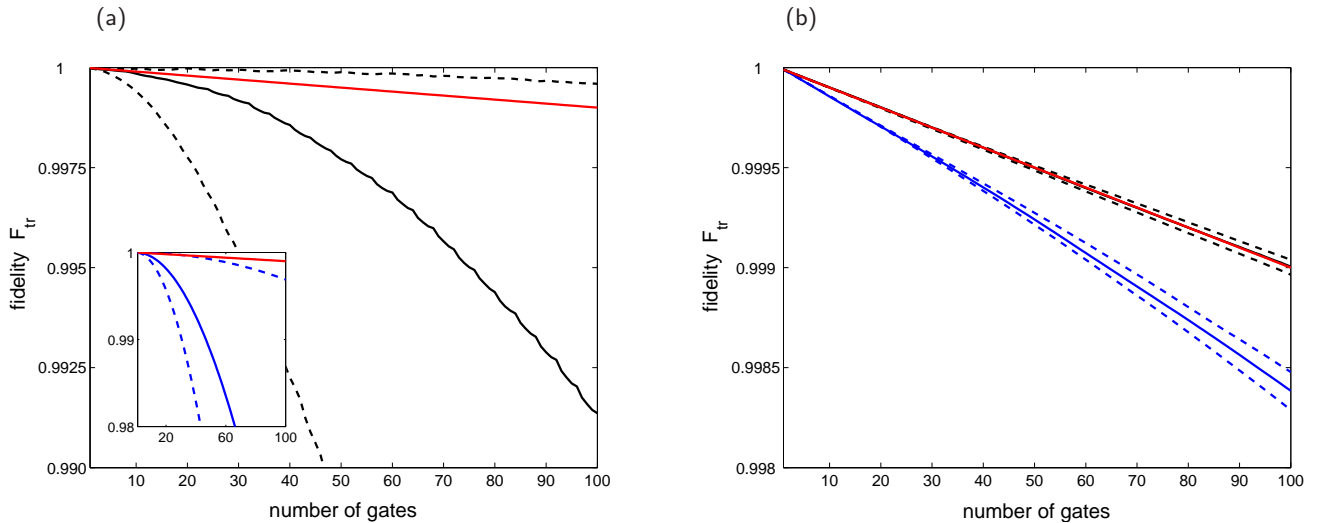


Figure 2: (Colour online) Comparison of error-propagation models for random unitary gates with $m = 2$ qubits (a) and $m = 8$ qubits (b). Single gate fidelity in the Monte Carlo simulations is $F_m = 0.99999$. Repetition of the same gate A (blue) is compared with repetitions of a sequence of four independent gates $ABCD$ (black). Out of 10 Monte Carlo simulations (details see text), the median (solid lines) as well as the best and worst cases (dashed lines) are given. The red solid lines denote independent error propagation $F_{tr} = (F_m)^r$. Large systems ($m = 8$) with several gates ($ABCD$) resemble independent error propagation almost perfectly, as in (b) the black and the red solid lines coincide.

Error Propagation and Relaxative Losses

As the main figure of merit we refer to a quality function

$$q = F_{tr} e^{-\tau/T_R} \quad (4)$$

resulting from the fidelity F_{tr} and the dissipative decay with overall relaxation rate constant T_R during a duration τ assuming independence of fidelity and decoherence. Moreover, for n qubits one defines as the trace fidelity of an experimental unitary module U_{exp} with respect to the target gate V_{target} (thus $U, V \in U(N)$ with $N := 2^n$)

$$\begin{aligned} F_{tr} &:= \frac{1}{N} \text{Re tr}\{V_{\text{target}}^\dagger U_{\text{exp}}\} \\ &= 1 - \frac{1}{2N} \|V_{\text{target}} - U_{\text{exp}}\|_2^2, \end{aligned} \quad (5)$$

which follows via the simple relation to the Euclidean distance

$$\begin{aligned} \|V - U\|_2^2 &= \|U\|_2^2 + \|V\|_2^2 - 2 \text{Re tr}\{V^\dagger U\} \\ &= 2N - 2N \frac{1}{N} \text{Re tr}\{V^\dagger U\} \\ &= 2N(1 - F_{tr}), \end{aligned}$$

the latter two identities invoking unitarity. The reason for choosing the trace fidelity is its convenient Fréchet differentiability in view of gradient-flow techniques, see also Ref. [24].

Consider an m -qubit-interaction module (CISC) with quality $q_m = F_m e^{-\tau_m/T_m}$ that decomposes into r universal two-qubit gates (RISC), out of which $r' \leq r$

gates have to be performed *sequentially*. Moreover, each 2-qubit gate shall be carried out with the uniform quality $q_2 = F_2 e^{-\tau_2/T_2}$. Henceforth we assume for simplicity equal relaxation rate constants, so $T_2 = T_m$ are identified with T_R . Then, as a first useful rule of the thumb and assuming independent error propagation, it is advantageous to compile the m -qubit module directly if $F_m > (F_2)^r$. Or more precisely taking relaxation into account, if the module can be realised with a fidelity

$$F_m > (F_2)^r e^{-(r' \cdot \tau_2 - \tau_m)/T_R}. \quad (6)$$

A more refined picture emerges from Monte-Carlo simulations of error propagation. To this end, compare the above independent error estimates with two scenarios for a sequence of r gates in total: (i) the r -fold repetition of single unitary gates A with individual errors meant to give A^r with $r = 1, 2, 3, \dots$ and (ii) the repetition of a sequence of four different gates A, B, C, D again each with individual errors to give $(D \circ C \circ B \circ A)^{r/4}$ where $r = 4, 8, 12, \dots$. In the sequel, we refer to case (i) as $AAAA$ and to case (ii) as $ABCD$.

For gates and errors to be generic, we use random unitaries (distributed according to the Haar measure following a recent modification [43] of the QR-algorithm). To a given random unitary m -qubit gate $A_0 \in U(2^m)$ (defining its Hamiltonian H_{A_0} via $A_0 = e^{-iH_{A_0}}$) we simulate a generic error as follows: from another independent unitary E_j take the matrix logarithm H_{A_j} such that $e^{-iH_{A_j}} = E_j$. Then to a given trace fidelity F , a corresponding unitary with a Monte-Carlo random error (the error being introduced on the level of the Hamiltonian

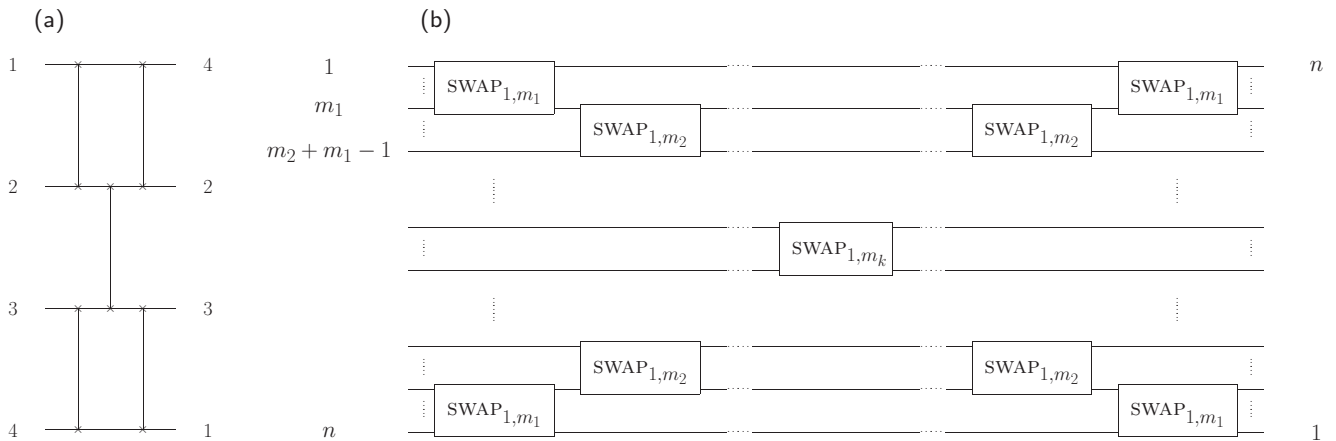


Figure 3: (a) Simple starting point: building a $\text{SWAP}_{1,4}$ gate from five $\text{SWAP}_{1,2}$. (b) Generalisation: assembling a $\text{SWAP}_{1,n}$ by four SWAP_{1,m_j} for each type $j = 1, 2, \dots, k-1$ and one single SWAP_{1,m_k} so that $m_k + 2 \sum_{j=1}^{k-1} (m_j - 1) = n$.

generators) can readily be obtained by solving

$$\begin{aligned} F &= 1 - \frac{1}{2N} \|A_0 - A_j\|_2^2 \\ &= 1 - \frac{1}{2N} \|A_0 - e^{-i(H_{A_0} + \delta \cdot H_{A_j})}\|_2^2 \end{aligned} \quad (7)$$

for $\delta > 0$. Along these lines one obtains the Monte-Carlo fidelities for repeating the A -gate by

$$F_{AAAA}(r) = 1 - \frac{1}{2N} \left\| (A_0)^r - \prod_{j=1}^r A_j \right\|_2^2 \quad (8)$$

and

$$F_{ABCD}(r) = 1 - \frac{1}{2N} \left\| (D_0 C_0 B_0 A_0)^{\frac{r}{4}} - \prod_{j=1}^{\frac{r}{4}} (D_j C_j B_j A_j) \right\|_2^2, \quad (9)$$

where the product runs from right to left. These Monte-Carlo simulations are compared to the simple model of independent errors according to

$$F_{\text{ind}} = (F_m)^r. \quad (10)$$

As shown in Fig. 2(a), for two-qubit gates the error propagates with a vast variance, which makes it virtually unpredictable. Thus assuming independence is always too optimistic for AAAA, while for ABCD it is still mostly optimistic, although there are cases in which the errors may compensate to give less effective loss than expected under independence.

However, when moving to effective multi-qubit gates, i.e., CISC modules, the generic situation becomes more predictable. For example, in 8-qubit random unitary gates, Fig. 2(b) shows that AAAA is significantly deviating from independent error propagation, whereas ABCD resembles independent error propagation almost perfectly. The situation is qualitatively exactly the same

even if the single gate error is larger as tested by analogous Monte-Carlo simulations setting $F_{\text{tr}} = 0.99$ or $F_{\text{tr}} = 0.96$ (not shown).

In the sequel, we will—for the sake of simplicity—often assume independent error propagation at the expense of systematically underestimating the pros of CISC compilation compared to the standard RISC compilation into universal local and two-qubit gates.

Computational Methods and Devices

Following the lines of our previous work on time complexity [24], we used the GRAPE algorithm [36] for direct CISC compilation. It tracks the fixed final times down to the shortest durations of controls still allowing for synthesising the unitary target gates with full fidelity. This gives currently the best known upper bounds to the minimal times required to realise a target module on a concrete hardware setting. We extended our parallelised C++ code of the GRAPE package described in [38] by adding more flexibility allowing to efficiently exploit available parallel nodes independent of internal parameters [44]. Moreover, faster algorithms for matrix exponentials on high-dimensional systems based on approximations by Tchebychev series have been developed [45] specifically in view of application to large quantum systems [44]. Thus computations could be performed on the HLRB-II supercomputer cluster at *Leibniz Rechenzentrum* of the Bavarian Academy of Sciences Munich. It provides an SGI Altix 4700 platform equipped with 9728 Intel Itanium2 Montecito Dual Core processors with a clock rate of 1.6 GHz, which give a total LINPACK performance of 63.3 TFlops/s. The present explorative study exploited the time allowance of approx. 500.000 CPU hours.

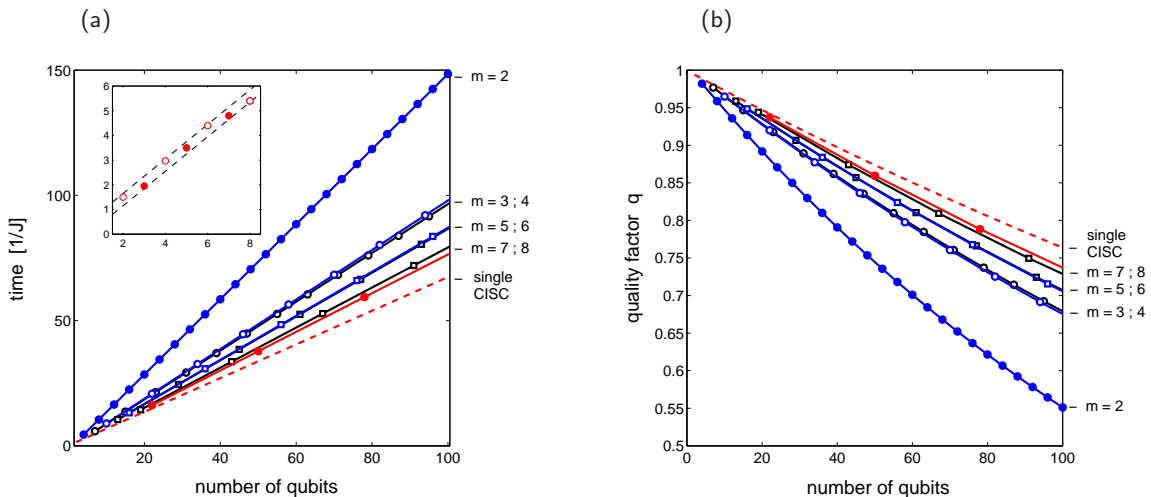


Figure 4: (Colour online) (a): Times required for indirect $\text{SWAP}_{1,n}$ on linear chains of n Ising-coupled qubits by assembling $\text{SWAP}_{1,m}$ building blocks reaching from $m = 2$ (RISC) up to $m = 8$ (CISC). Using linear regression, the dashed line is an extrapolation of the direct single-CISC compilations shown in the inset to large number of qubits, where direct CISC compilation is virtually impossible on classical computers. Time units are expressed as $1/J_{ZZ}$ assuming the duration of local operations can be neglected compared to coupling evolutions (details in the text). (b): Translation of the effective gate times into overall quality figures $q = (q_m)^{r_m}$ for an effective gate assembled from r_m components of single qualities $q_m := F_m e^{-\tau_m/T_R}$ (with the respective component fidelities homogeneously falling into a narrow interval $F_m \in [0.99994, 0.99999]$ for $m = 3, \dots, 8$). Data are shown for a uniform relaxation rate constant of $1/T_R = 0.04J_{ZZ}$.

I. THE $1, n$ SWAP OPERATION

The easiest and most basic examples to illustrate the pertinent effects of optimal-control based CISC-quantum compilation are the respective indirect $\text{SWAP}_{1,n}$ gates in spin chains of n qubits coupled by nearest-neighbour Ising interactions with J_{ZZ} denoting the coupling constant.

For the $\text{SWAP}_{1,2}$ unit there is a standard textbook decomposition into three CNOTs. Thus for Ising-coupled systems and in the limit of fast local controls, the total time required for an $\text{SWAP}_{1,2}$ is $3/(2J_{ZZ})$, and there is no faster implementation [46, 47]. Note, however, that in systems coupled by the isotropic Heisenberg interaction XXX , the $\text{SWAP}_{1,2}$ may be directly implemented just by letting the system evolve for a time of only $1/(2J_{XXX})$. Sacrificing universality, it may thus be advantageous to regard the $\text{SWAP}_{1,2}$ as basic unit for the $\text{SWAP}_{1,n}$ task rather than the universal CNOT. Clearly, any even-order $\text{SWAP}_{1,2n}$ can be built from $\text{SWAP}_{1,2}$ along the lines of the most obvious scheme of Fig. 3(a). (The odd-order $\text{SWAP}_{1,2n-1}$ follow, e.g., from $\text{SWAP}_{1,2n}$ by omitting qubit $2n$ and all the gates connected to it.)

Moreover, the generalisation to decomposing a $\text{SWAP}_{1,n}$ into a sequence with k different SWAP_{1,m_j} building blocks (where $j = 1, 2, \dots, k$) as shown in Fig. 3(b) is straightforward by ensuring $m_k + 2 \sum_{j=1}^{k-1} (m_j - 1) = n$. Due to its symmetry, the total duration then amounts to

$$\tau(\text{SWAP}_{1,n}) = \tau(\text{SWAP}_{1,m_k}) + 2 \sum_{j=1}^{k-1} \tau(\text{SWAP}_{1,m_j}) \quad (11)$$

and the fidelity reads

$$F(\text{SWAP}_{1,n}) = F(\text{SWAP}_{1,m_k}) \prod_{j=1}^{k-1} F(\text{SWAP}_{1,m_j})^4 \times e^{-\tau(\text{SWAP}_{1,n})/T_R} \quad (12)$$

Now, the SWAP_{1,m_j} building blocks themselves can be precompiled into time-optimised single complex instruction sets by exploiting the GRAPE-algorithm of optimal control up to the current limits of m_j imposed by CPU-time allowance.

Proceeding in the next step to large n , Fig. 4 underscores how the time required for $\text{SWAP}_{1,n}$ gates decreases significantly by assembling precompiled SWAP_{1,m_j} building blocks as CISC units recursively up to a multi-qubit interaction size of $m_j = 8$, where the speed-up is by a factor of more than 1.96. Clearly, such a set of SWAP_{1,m_j} building blocks with $m_j \in \{2, 3, 4, 5, 6, 7, 8\}$ allows for efficiently synthesising any $\text{SWAP}_{1,n}$. Assuming for the moment that a linear time complexity of the $\text{SWAP}_{1,n}$ can be taken for granted, one may extrapolate the results of direct CISC compilation from the range of the inset of Fig. 4(a) to a large number of qubits. One thus obtains an estimated upper limit to the time complexity of the $\text{SWAP}_{1,n}$. This is indicated by the dashed line, the slope of which will be defined as Δ_∞ . Likewise, the irrespective slopes of the m -qubit decomposition are denoted by Δ_m .

With these stipulations, we introduce as a measure for the potential of CISC compilation (versus RISC compila-

tion) the ratio of the slopes

$$\pi_{\text{CISC}} := \frac{\Delta_2}{\Delta_\infty} \quad (13)$$

and as a measure for the extent to which this potential has been exhausted by m -qubit CISC compilation the ratio

$$\eta_m := \frac{\Delta_\infty}{\Delta_m} \quad (14)$$

thus providing as convenient measure of improvement

$$\xi_m := \frac{\Delta_2}{\Delta_m} = \eta_m \cdot \pi_{\text{CISC}} \quad (15)$$

The data of Fig. 4 thus give a potential of $\pi_{\text{CISC}} = 2.16$; by $m = 8$ -qubit interactions it is already pretty well exhausted, as inferred from $\eta_8 = 0.87$. The current CISC over RISC improvement then amounts to $\xi_8 = 1.88$.

On the other hand, deducing from Fig. 4 right away that the time complexity of $\text{SWAP}_{1,n}$ ought to be linear would be premature: although the slopes seem to converge to a non-zero limit, numerical optimal control may become systematically inefficient for larger interaction sizes m . Therefore, although improbable, e.g., convergence of the slopes to a value of zero cannot be safely excluded on the current basis of findings. This also means a logarithmic time complexity can ultimately not be excluded either.

Summarising the results for the indirect SWAPs in terms of the three criteria described in the introduction, we have the following: (i) in Ising coupled qubit chains, there is no speed-up by changing the basic unit from the universal CNOT into a $\text{SWAP}_{1,2}$, whereas in isotropically coupled systems the speed-up amounts to a factor of three; (ii) extending the building blocks of $\text{SWAP}_{1,m}$ from $m = 2$ (RISC) to $m = 8$ (CISC) gives a speed-up by a factor of nearly two (1.96) even under Ising-type couplings; (iii) the numerical data are consistent with a time complexity converging to a linear limit for the $\text{SWAP}_{1,n}$ task in Ising chains, however, there is no proof for it yet.

II. THE QUANTUM FOURIER TRANSFORM (QFT)

Since many quantum algorithms take advantage of efficiently solving some hidden subgroup problem, the quantum Fourier transform plays a central role [6, 7, 8].

In order to realise a QFT on large qubit systems, our approach is the following: given an m -qubit QFT, we show that for obtaining a $(k \cdot m)$ -qubit QFT by recursively using multi-qubit building blocks, a second type of module is required, to wit a combination of controlled phase gates and SWAPs, which henceforth we dub m' -qubit cP-SWAP for short.

Here we present two alternatives: variant I with $m' = 2m$ and, as a special case, variant II for even $m' = m$.

Choosing $m = 2$ and $k = 3$ for a start, the recursive construction is illustrated in Fig. 5. The top trace shows the standard textbook realisation of a 6-qubit QFT. By shifting the final SWAP operations, it can be rearranged into the sequence of gates depicted in the lower trace. Note that the gates appearing in solid boxes constitute a $2m$ -qubit QFT (which itself is made of two m -qubit QFTs and a central m -qubit cP-SWAP), while the ones in dashed boxes have to be added for a $3m$ -qubit QFT. For $m = 2$ we have thus shown how a $3m$ -qubit QFT reduces to a $2m$ -qubit QFT, two $2m$ -qubit cP-SWAPs, and an m -qubit QFT. So with $2m$ providing a foundation, at the same time we have also illustrated the induction from a $k \cdot m$ -QFT to a $(k + 1) \cdot m$ -QFT. Moreover, the same construction principle holds for any block size $m = 2, 3, \dots$, which can readily be proven by a straightforward, but lengthy induction from m to $m + 1$.

One thus arrives at the desired block decomposition of a general $(k \cdot m)$ -qubit QFT as shown in Fig. 6 (which is variant I; the less effective variant II can be found in Appendix A): it requires k times the same m -qubit QFT interdispersed with $\binom{k}{2}$ times an $2m$ -qubit cP-SWAP, out of which $k - 1$ show different phase-rotation angles. For all m and $j = 1, 2, \dots, (k - 1)$, one finds the following observations:

1. a cP-SWAP $_{2m}^j$ takes as least as long as a QFT $_m$;
2. a QFT $_m$ takes as least as long as a cP-SWAP $_m^j$;
3. a cP-SWAP $_m^j$ takes least as long as a cP-SWAP $_m^{j+1}$.

Thus the duration of a $(k \cdot m)$ -qubit QFT built from m -qubit and $2m$ -qubit modules amounts to

$$\tau(\text{QFT}_{k \cdot m}) = 2 \cdot \tau(\text{QFT}_m) + (k - 1) \cdot \tau(\text{cP-SWAP}_{2m}^1) + (k - 2) \cdot \tau(\text{cP-SWAP}_{2m}^2) \quad (16)$$

Next, consider the overall quality of a $(k \cdot m)$ -qubit QFT in terms of its two types of building blocks, namely the basic m -qubit QFT as well as the constituent $2m$ -qubit cP-SWAPs with their respective different rotation angles. It reads

$$q_{\text{QFT}_{k \cdot m}} = (F_{\text{QFT}_m})^k \left(\prod_{j=1}^{k-1} (F_{\text{cP-SWAP}_{2m}^j})^{k-j} \right) \times e^{-(\tau_{\text{QFT}_{k \cdot m}}/T_R)} \quad (17)$$

In the following, we will neglect rotations as soon as their angle falls short of a threshold of $\pi/2^{10}$. This approximation is safe since it is based on a calculation of a 20-qubit QFT, where the truncation does not introduce any relative error beyond 10^{-5} . According to the block decomposition of Fig. 6, thus three instances of cP-SWAPs are left, since all cP-SWAP $_{10}^j$ elements with $j \geq 3$ boil down to mere SWAP gates due to truncation of small rotation angles. The representation of these cP-SWAP modules is shown in Appendix B as Fig. 12.

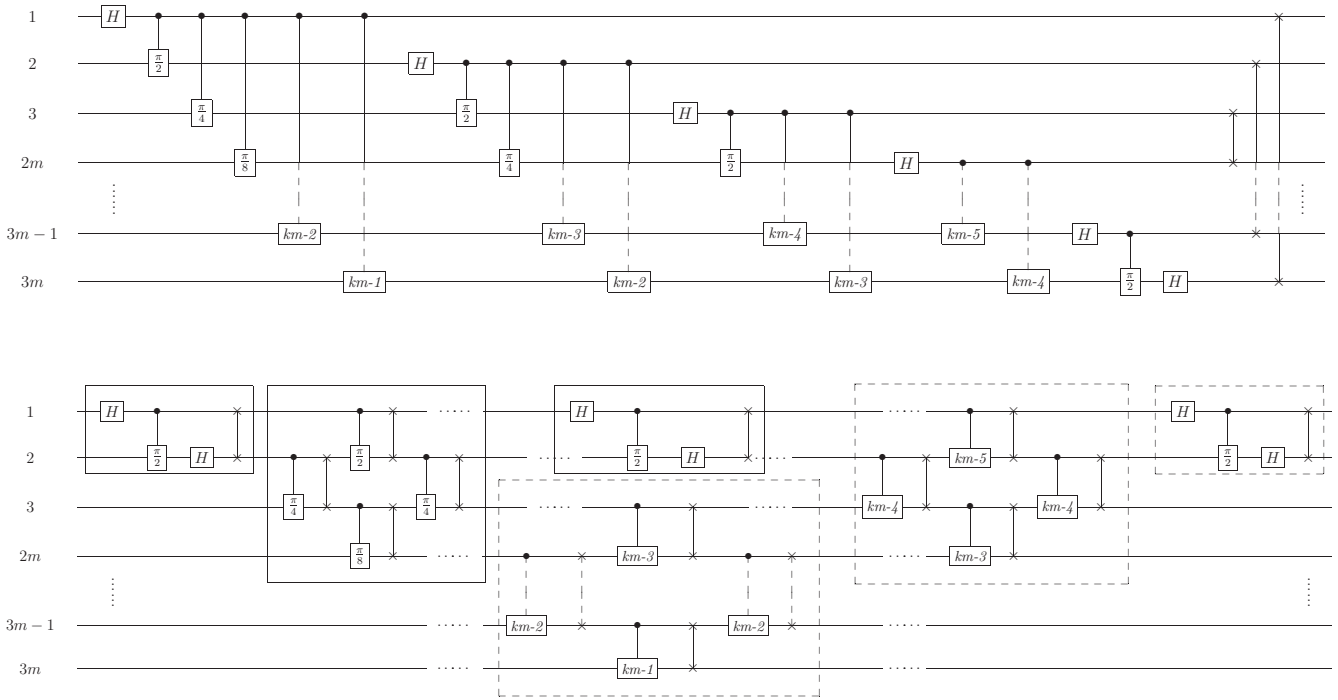


Figure 5: By rearranging the SWAPs and controlled phase gates, the standard decomposition of a $3m$ -qubit quantum Fourier transform, QFT (top trace) reduces to a realisation adapted to a coupling topology of linear nearest-neighbour interactions (lower trace) with a $2m$ -qubit QFT, m -qubit cP-SWAPs (solid boxes), and an m -qubit QFT (dashed box). The notation $(km - \nu)$ is a shorthand for a rotation angle of $\phi = \frac{\pi}{2^{km-\nu}}$.

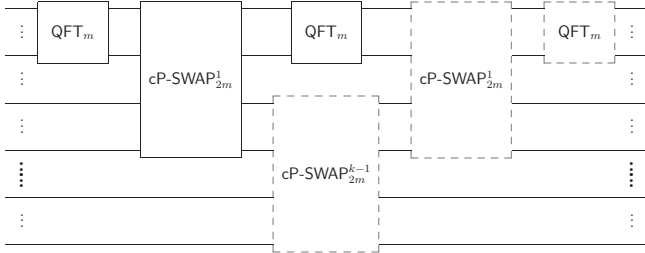


Figure 6: For $k \geq 2$, a (km) -qubit QFT can be assembled from k times an m -qubit QFT and $\binom{k}{2}$ instances of $2m$ -qubit modules cP-SWAP_{2m}^j , where the index j of different phase-rotation angles takes the values $j = 1, 2, \dots, k-1$. The dashed boxes correspond to Fig. 5 and show the induction $k \mapsto k+1$.

With these stipulations, we address the task of assembling an $(k \cdot 10)$ -qubit QFT, exploiting the limits of current allowances on the HLRB-II cluster. This translates into using 10-qubit cP-SWAP building blocks ($2m = 10$) and the 5-qubit QFT ($m = 5$) in the sense of a $(2k \cdot 5)$ -qubit QFT. Its duration $\tau(\text{QFT}_{2k \cdot 5})$ is readily obtained as in Eqn. 16 thus giving an overall quality of

$$q_{\text{QFT}_{2k \cdot 5}} = (F_{\text{QFT}_5})^{2k} (F_{\text{cP-SWAP}_{10}^1})^{2k-1} (F_{\text{cP-SWAP}_{10}^2})^{2k-2} \times (F_{\text{cP-SWAP}_{10}^3})^{\binom{2k}{2}-4k+3} e^{-\tau_{\text{QFT}_{2k \cdot 5}}/T_R}. \quad (18)$$

Based on this relation, the numerical results of Fig. 7 show that a CISC-compiled QFT is moderately superior to the standard RISC versions [48, 49]. Although the potential of CISC compilation amounts to $\pi_{\text{CISC}} = 2.27$, recursively assembling 5-qubit QFTs and 10-qubit cP-SWAPs only exploits about half of it as apparent in the value of $\eta_{5,10} = 0.53$.

As has been pointed out by Zeier [50], the decomposition of a many-qubit QFT into smaller QFTs and concatenations of a permutation matrix and a diagonal matrix roots back in a principle already used in the Cooley-Tukey algorithm [9] for the discrete Fourier transform (DFT): Let $N = m \cdot q$. Then one obtains [51, 52]

$$\begin{aligned} \text{DFT}_N &= L \circ (\text{DFT}_m \otimes \mathbb{1}_q) \circ D \circ (\mathbb{1}_m \otimes \text{DFT}_q) \\ &= (\mathbb{1}_q \otimes \text{DFT}_m) \circ (L' \circ D) \circ (\mathbb{1}_m \otimes \text{DFT}_q), \end{aligned} \quad (19)$$

where $L, L' \in \text{Mat}_N$ are permutation matrices. Moreover, setting $\omega := e^{2\pi i/N}$, the diagonal matrix takes the form

$$D = \text{diag}(\omega^{tk} | t_k = (k \bmod m) \lfloor \frac{k}{m} \rfloor \text{ for } k = 0, 1, 2, \dots, N-1) \quad (20)$$

Therefore, the QFT decompositions made use of here exactly follow the classical scheme in the second line of Eqn. 19: the expression $(L' \circ D)$ corresponding to the cP-SWAP.

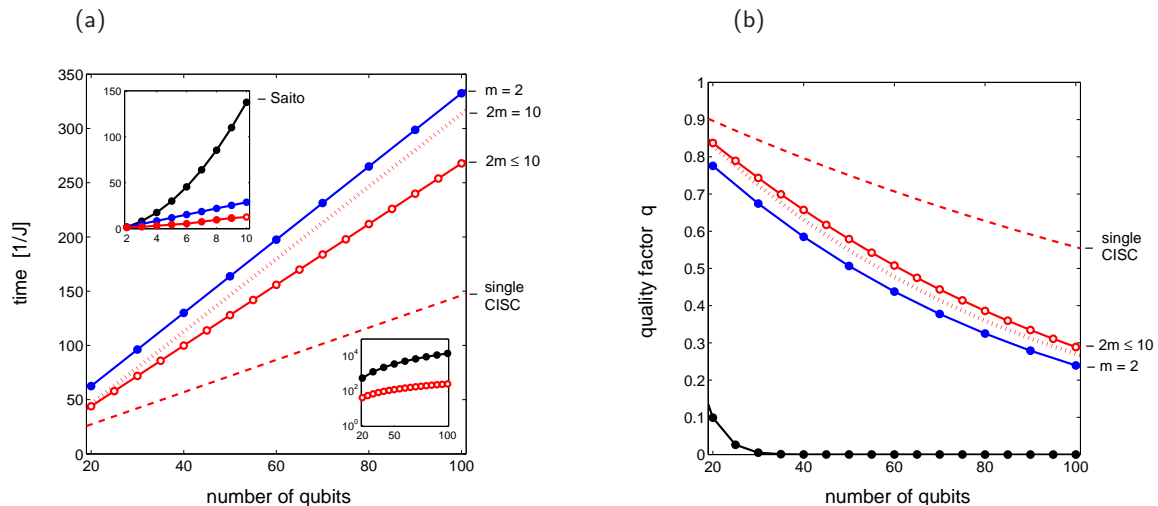


Figure 7: (Colour online) Comparison of CISC-compiled QFT (red) with standard RISC compilations ($m = 2$) following the scheme by Saito [48] (black) or Blais [49] (blue): (a) times for implementation translate into quality factors (b) for a relaxation rate constant of $1/T_R = 0.04J_{ZZ}$. Again, the dashed red line extrapolates from the direct single-CISC compilations shown in the upper inset of (a), the lower inset giving in logarithmic scales the times needed for the standard textbook RISC compilation ($m = 2$) on a linear Ising chain. Dotted red lines represent the less favourable results from QFT variant II (Appendix A).

III. THE MULTIPLE-CONTROLLED NOT GATE (C^n NOT)

Multiply-controlled CNOT gates generalise Toffoli's gate. Here, we move from C^2 NOT to C^{n-2} NOT in an n -qubit system with one ancilla and one target qubit. The reason for the ancilla qubit being that it turns the problem to linear complexity [53]. Moreover, in view of realistic large systems, we assume again a topology of a linear chain coupled by nearest-neighbour Ising interactions. Since CNOT-gates frequently occur in error-correction schemes, they are highly relevant in practice.

Here we address the task of decomposing a C^{n-2} NOT into lower CNOTs and indirect SWAP gates (see Sec. I).

To this end, we will generalise the basic principle of reducing a C^n NOT to C^m NOT gates with $m < n$ that can be demonstrated by decomposing a C^3 NOT into Toffoli gates according to scheme of Fig. 8 devised by Barenco *et al.* in [53]. Starting with any of the 2^5 computational basis states $|x_1, x_2, x_3, x_4, x_5\rangle$ (where $x_k \in \{0, 1\}$, \oplus denotes addition mod 2, and $x_k x_\ell$ being the usual scalar product) track the effect of the gate sequentially from state $|a\rangle$ through state $|e\rangle$

$$\begin{aligned}
 |a\rangle &= |x_1, x_2, x_3, x_4, x_5\rangle \\
 |b\rangle &= |x_1, x_2, x_3 \oplus x_1x_2, x_4, x_5\rangle \\
 |c\rangle &= |x_1, x_2, x_3 \oplus x_1x_2, x_4, x_5 \oplus x_4(x_3 \oplus x_1x_2)\rangle \\
 &= |x_1, x_2, x_3 \oplus x_1x_2, x_4, x_5 \oplus x_4x_3 \oplus x_1x_2x_4\rangle \\
 |d\rangle &= |x_1, x_2, x_3 \oplus x_1x_2 \oplus x_1x_2, x_4, x_5 \oplus x_4x_3 \oplus x_1x_2x_4\rangle \\
 &= |x_1, x_2, x_3, x_4, x_5 \oplus x_4x_3 \oplus x_1x_2x_4\rangle \\
 |e\rangle &= |x_1, x_2, x_3, x_4, x_5 \oplus x_4x_3 \oplus x_4x_3 \oplus x_1x_2x_4\rangle \\
 &= |x_1, x_2, x_3, x_4, x_5 \oplus x_1x_2x_4\rangle
 \end{aligned}$$

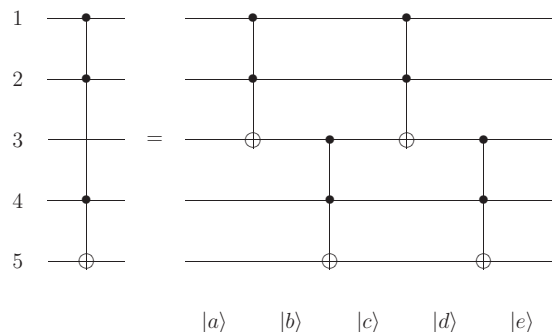


Figure 8: Decomposition of a C^3 -NOT with one ancilla qubit into four C^2 -NOTs (Toffoli gates) according to ref. [53]. States $|a\rangle$ through $|e\rangle$ are explained in the text.

to see the overall effect of the gate sequence is a C^3 NOT thus proving the decomposition.

Fig. 9 provides a generalisation of the scheme in Fig. 8: in the first place (a), the number of control qubits is reduced by introducing k blocks with m_3 qubits that are left invariant. The price for this reduction is a four-fold occurrence of the reduced building blocks. In the second step (b), the reduced building blocks are expanded into a sequence with two central C^{m_2} NOTs, two terminal $C^{(m_3+1)}$ NOTs and two lots of $2(k-1)$ times $C^{(m_3+1)}$ NOT each. For $k = 4, 5, 6, \dots$ part (a) and (b) can be expanded in a general concatenated way thus entailing an

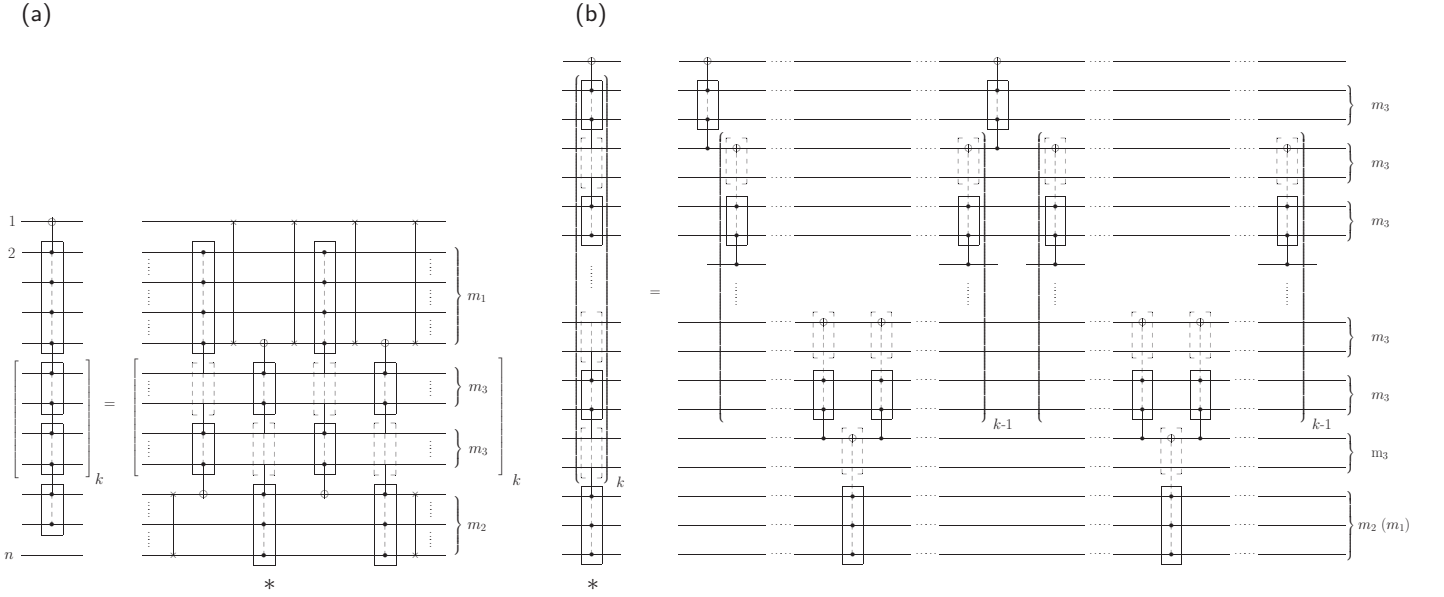


Figure 9: Decomposition of a C^{n-2} NOT gate on a linear coupling topology: (a) reduction of the number of control qubits to four intermediate gates with less control qubits and (b) decomposition of the intermediate multiply-controlled NOT-gate appearing in (a). In an n -qubit system, there is one target qubit, one ancilla qubit and $n-2$ control qubits; so $m_1 + (m_2 - 1) + 2km_3 = n-2$ with $m_1, m_3 \geq 1$ and $m_2 \geq 2$. Read the brackets $[\cdot]_k$ in (a) as *to be repeated k times* and $(\cdot)_k$ in (b) as *expanded k -fold*.

overall duration of

$$\begin{aligned}
\tau(C^{n-2}\text{NOT})\Big|_{k \geq 4} &= 4\tau(C^{m_1}\text{NOT}) \\
&+ 4\tau(C^{m_2}\text{NOT}) + \tau(\text{SWAP}_{1,m_2}) \\
&+ (13k - 8)\tau(C^{m_3+1}\text{NOT}) \\
&+ (1 - \delta_{m_3,1}) (13k + 3)\tau(\text{SWAP}_{1,m_3}) .
\end{aligned} \tag{21}$$

For completeness, note that the cases $k = 3, 2, 1$ have to be treated separately, since they only allow for less and less densely concatenated expansions (not shown). Their respective durations are

$$\begin{aligned}
\tau(C^{n-2}\text{NOT})\Big|_{k=1} &= 4\tau(C^{m_1}\text{NOT}) + 2\tau(\text{SWAP}_{1,m_1+1}) \\
&+ 4\tau(C^{m_2}\text{NOT}) + 2\tau(\text{SWAP}_{1,m_2}) \\
&+ 8\tau(C^{m_3+1}\text{NOT}) + (1 - \delta_{m_3,1}) 16\tau(\text{SWAP}_{1,m_3})
\end{aligned} \tag{22}$$

$$\begin{aligned}
\tau(C^{n-2}\text{NOT})\Big|_{k=2} &= 4\tau(C^{m_1}\text{NOT}) \\
&+ 4\tau(C^{m_2}\text{NOT}) + \tau(\text{SWAP}_{1,m_2}) \\
&+ 24\tau(C^{m_3+1}\text{NOT}) + (1 - \delta_{m_3,1}) 32\tau(\text{SWAP}_{1,m_3})
\end{aligned} \tag{23}$$

$$\begin{aligned}
\tau(C^{n-2}\text{NOT})\Big|_{k=3} &= 4\tau(C^{m_1}\text{NOT}) \\
&+ 4\tau(C^{m_2}\text{NOT}) + \tau(\text{SWAP}_{1,m_2}) \\
&+ 37\tau(C^{m_3+1}\text{NOT}) + (1 - \delta_{m_3,1}) 48\tau(\text{SWAP}_{1,m_3}) .
\end{aligned} \tag{24}$$

However, the total number of gates only depends on $k = 1, 2, 3, \dots$, so that obtains as the overall quality

$$\begin{aligned}
q\Big|_k &= (F_{C^{m_1}\text{NOT}})^4 (F_{\text{SWAP}_{1,m_1+1}})^4 \\
&\times (F_{C^{m_2}\text{NOT}})^4 (F_{\text{SWAP}_{1,m_2}})^2 \\
&\times (F_{C^{m_3+1}\text{NOT}})^{16k-8} (F_{\text{SWAP}_{1,m_3}})^{(1-\delta_{m_3,1})16k} \\
&\times e^{-\tau(C^{n-2}\text{NOT})\Big|_k / T_R} .
\end{aligned} \tag{25}$$

Given the duration of the decomposition as in Eqn. 21, it is easy to see that implementing the m_1 control qubits comes with the lowest time weight (4) and without a time overhead of auxiliary gates. Implementing the m_2 control qubits, however, requires the same time weight (4), but entails the time for one auxiliary SWAP_{1,m_2} gate. In order to implement the $k \cdot m_3$ control qubits, in turn, a sizeable amount of auxiliary SWAPs are needed.

Therefore, whenever high fidelities can be reached (so that the quality is limited by decoherence not by fidelity), a good strategy of combining the expansive decomposition in Fig. 9(a) with the recursive decomposition in part (b) is the following: given $n-2$ control qubits and with the current limitation from direct CISC compilation being $m_j \leq 9$, choose m_1 to be the largest, m_2 to be the second largest and such that one obtains an even number for $n - m_1 - m_2 - 1 = 2km_3$.

In the next step, a decision has to be made in order to minimise the contributions in the last line of Eqn. 21, whenever there are several integer solutions $k_1 m_{31} = k_2 m_{32}$. So for integer $k \geq 4$, this amounts

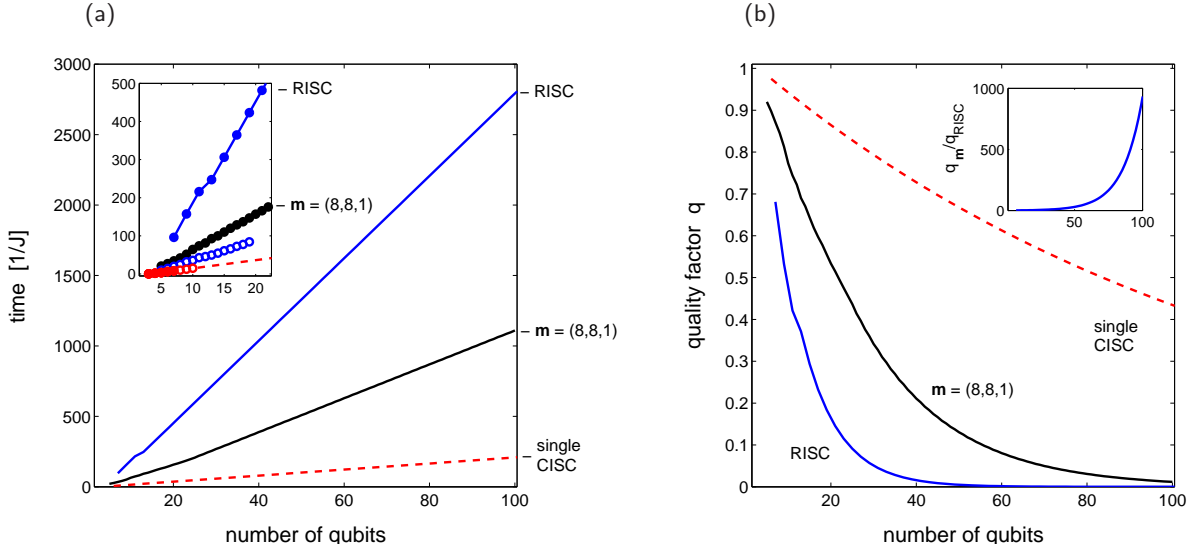


Figure 10: (Colour online) Comparing implementations of C^{n-2} NOTs on a linear Ising spin chain using CNOT and SWAP_{1,2} modules for the RISC compilation or multi-qubit building blocks according to the CISC assembler scheme of Fig. 9. As a shorthand, the different numbers of control qubits are expressed by $\mathbf{m} := (m_1, m_2, m_3)$. Using the expansion of Fig. 9, the CISC results (black solid lines) are obtained for $k = 4, 5, 6, \dots$ with $m_1 = 8$ and $m_2 = 8$ (for odd n) or $m_2 = 7$ (for even n), while $m_3 = 1$ thus ensuring $m_1 + (m_2 - 1) + 2km_3 = n - 2$. The red dotted line extrapolates again the direct CISC results beyond 10 qubits. In (a) deviations from straight lines occur, as the cases $k = 1, 2, 3$ follow special concatenation patterns (see text), while $k = 4, 5, 6, \dots$ are generic. The inset in (a) also shows results of a non-scalable recursive expansion that is confined up to 19 qubits (blue circles).

to the ordinary optimisation task

$$\begin{aligned} \min_k (13k - 8) \{ (m_3 + 2)\Delta_C + a \} \\ + (1 - \delta_{m_3,1}) (13k + 3) \{ m_3\Delta_S + b \} \\ \text{subject to: } km_3 = c \equiv \text{const.} \end{aligned} \quad (26)$$

Here we approximate the times for a C^{m_3+1} NOT by the linear expression $\tau(C^{m_3+1}\text{NOT}) = (m_3 + 2)\Delta_C + a$ and likewise for the SWAP_{1, m_3} by $\tau(\text{SWAP}_{1,m_3}) = m_3\Delta_S + b$ with the values for the slopes Δ_C and Δ_S as well for the offsets a and b being taken from the respective linear extrapolation Δ_∞ for direct CISC compilation ($\Delta_C^{(\infty)} = 2.15$ and $\Delta_S^{(\infty)} = 0.69$ as well as $a = -4.48$ and $b = 0.06$). In the setting of these parameters, Eqn. 21 implies it is timewise advantageous to choose as the decomposition of the interior block in Fig. 9(b) the counter-intuitive option with a large number of repetitions k and small block sizes m_3 . This is because in the above parameter setting, the duration takes its minimum on the margin of high repetitions k and smallest block sizes $m_3 = 1$ corresponding to Toffoli gates thus circumventing the overhead skipped by $(1 - \delta_{m_3,1}) = 0$.

IV. CONCLUSIONS

We have exploited the power of a cutting-edge high-performance parallel cluster for quantum CISC compilation. Thus the standard toolbox of universal quantum gate modules (RISC) has been extended by time-optimised effective multi-qubit gates (CISC). We have shown ways how these CISC modules can be assembled in a scalable way in order to address large-scale quantum computing on systems that are too large for direct CISC compilation. Although our optimal-control based CISC-compilation routine exploits parallel matrix operations for clusters as well as fast matrix exponentials [44], increasing the system size by one qubit roughly requires a factor of eight more CPU time. Since direct CISC compilation thus scales exponentially, scalable assembler schemes for multi-qubit CISC modules are needed, and we have presented some elementary ones:

For indirect SWAPS, the quantum Fourier transform, and multiply-controlled NOT-gates, the CISC decomposition is significantly faster than the standard RISC decomposition into local plus universal two-qubit gates. The current improvements range from 20% up to a speed-up by nearly a factor of 2.5. However, as illustrated in Tab. I, the potential of CISC compilation is by far not yet exhausted with the current results. Thus although the CISC compiler already provides a powerful means to fight decoherence, more refined optimisation in particular on the assembler level will be a frontier of future

Table I: Current Exploitation vs. Potential of Quantum CISC Compilation

gate	CISC potential:	estimate $\pi_{\text{CISC}} = \Delta_2/\Delta_\infty$	current status:	exploitation $\eta_m = \Delta_\infty/\Delta_m$	improvement $\xi_m = \Delta_2/\Delta_m$
SWAP _{1,n}	medium	2.16	fairly exhausted	0.86 [$m = 8$]	1.88
n -QFT	medium	2.27	halfway exhausted	0.53 [$\mathbf{m} = (5_{\text{QFT}}, 10_{\text{CP-SWAP}})$]	1.20
C^{n-2} NOT	big	13.6	not yet exhausted	0.18 [$\mathbf{m} = (8, 8, 1)_{n \text{ odd}}$ or $(8, 7, 1)_{n \text{ even}}$]	2.45

research. Using decoherence or error-protected modules as in ref. [34] will open the door to fault-tolerant CISC modules.

As a side effect, we have shown that gate errors in multi-qubit CISC modules propagate more favourably than in RISC modules confined to two-qubit gates.

This paves the way to another frontier of research: optimising the quantum assembler task on the extended toolbox of quantum CISC-modules with effective many-qubit interactions. Finally, it is to be anticipated that methods developed in classical computer science can also be put to good use for systematically optimising quantum assemblers.

Acknowledgments

This work was supported in part by the integrated EU project QAP and by *Deutsche Forschungsgemeinschaft*, DFG, within the incentive SFB-631. Access to the high-performance parallel cluster HLRB-II at *Leibniz Rechenzentrum* of the Bavarian Academy of Science is gratefully acknowledged. We wish to thank Matthias Christandl and Robert Zeier for fruitful discussions.

-
- [1] R. P. Feynman, *Int. J. Theo. Phys.* **21**, 467 (1982).
[2] R. P. Feynman, *Feynman Lectures on Computation* (Perseus Books, Reading, MA., 1996).
[3] P. W. Shor, in *Proceedings of the Symposium on the Foundations of Computer Science, 1994, Los Alamitos, California* (IEEE Computer Society Press, New York, 1994), pp. 124–134.
[4] P. W. Shor, *SIAM J. Comput.* **26**, 1484 (1997).
[5] C. H. Papadimitriou, *Computational Complexity* (Addison Wesley, Reading, MA., 1995).
[6] R. Jozsa, *Proc. R. Soc. A.* **454**, 323 (1998).
[7] R. Cleve, A. Ekert, C. Macchiavello, and M. Mosca, *Proc. R. Soc. A.* **454**, 339 (1998).
[8] M. Ettinger, P. Høyer, and E. Knill, *Inf. Process. Lett.* **91**, 43 (2004).
[9] J. W. Cooley and J. W. Tukey, *Math. Comput.* **19**, 297 (1965).
[10] T. Beth, *Verfahren der schnellen Fourier-Transformation* (Teubner, Stuttgart, 1984).
[11] S. Lloyd, *Science* **273**, 1073 (1996).
[12] D. Abrams and S. Lloyd, *Phys. Rev. Lett.* **79**, 2586 (1997).
[13] C. Zalka, *Proc. R. Soc. London A* **454**, 313 (1998).
[14] C. Bennett, I. Cirac, M. Leifer, D. Leung, N. Linden, S. Popescu, and G. Vidal, *Phys. Rev. A* **66**, 012305 (2002).
[15] L. Masanes, G. Vidal, and J. Latorre, *Quant. Inf. Comput.* **2**, 285 (2002).
[16] E. Jané, G. Vidal, W. Dür, P. Zoller, and J. Cirac, *Quant. Inf. Computation* **3**, 15 (2003).
[17] D. Deutsch, *Proc. Royal Soc. London A* **400**, 97 (1985).
[18] J. Dodd, M. Nielsen, M. Bremner, and R. Thew, *Phys. Rev. A* **65**, 040301(R) (2002).
[19] M. Bremner, D. Bacon, and M. Nielsen, *Phys. Rev. A* **71**, 052312 (2005).
[20] G. Vidal, K. Hammerer, and J. I. Cirac, *Phys. Rev. Lett.* **88**, 237902 (2002).
[21] A. M. Childs, H. L. Haselgrove, and M. A. Nielsen, *Phys. Rev. A* **68**, 052311 (2003).
[22] R. Zeier, M. Grassl, and T. Beth, *Phys. Rev. A* **70**, 032319 (2004).
[23] P. Wocjan, D. Janzing, and T. Beth, *Quant. Inf. Comput.* **2**, 117 (2002).
[24] T. Schulte-Herbrüggen, A. K. Spörl, N. Khaneja, and S. J. Glaser, *Phys. Rev. A* **72**, 042331 (2005).
[25] V. Ramakrishna and H. Rabitz, *Phys. Rev. A* **54**, 1715 (1995).
[26] T. Schulte-Herbrüggen, *Aspects and Prospects of High-Resolution NMR* (PhD Thesis, Diss-ETH 12752, Zürich, 1998).
[27] S. J. Glaser, T. Schulte-Herbrüggen, M. Sieveking, O. Schedletsky, N. C. Nielsen, O. W. Sørensen, and C. Griesinger, *Science* **280**, 421 (1998).
[28] U. Helmke, K. Hüper, J. B. Moore, and T. Schulte-Herbrüggen, *J. Global Optim.* **23**, 283 (2002).
[29] R. R. Tucci (1999), e-print: <http://arXiv.org/pdf/quant-ph/9902062>.
[30] D. Williams, *Quantum Computer Architecture, Assembly Language and Compilation* (Master’s Thesis, University of Warwick, 2004).
[31] V. V. Shende, S. Bullock, and I. L. Markov, *IEEE Trans. Comput.-Aided Des. Integr. Circuits Syst.* **25**, 1000 (2006).
[32] K. M. Svore, A. V. Aho, A. W. Cross, I. Chuang, and

- I. L. Markov, *Computer* **25**, 74 (2006).
- [33] R. R. Tucci (2007), e-print: <http://arXiv.org/0706.0479>.
- [34] T. Schulte-Herbrüggen, A. Spörl, N. Khaneja, and S. Glaser (2006), e-print: <http://arXiv.org/pdf/quant-ph/0609037>.
- [35] G. D. Sanders, K. W. Kim, and W. C. Holton, *Phys. Rev. A* **59**, 1098 (1999).
- [36] N. Khaneja, T. Reiss, C. Kehlet, T. Schulte-Herbrüggen, and S. J. Glaser, *J. Magn. Reson.* **172**, 296 (2005).
- [37] A. K. Spörl, T. Schulte-Herbrüggen, S. J. Glaser, V. Bergholm, M. J. Storcz, J. Ferber, and F. K. Wilhelm, *Phys. Rev. A* **75**, 012302 (2007).
- [38] T. Gradl, A. K. Spörl, T. Huckle, S. J. Glaser, and T. Schulte-Herbrüggen, *Lect. Notes Comput. Sci.* **4128**, 751 (2006), Proceedings of the EURO-PAR 2006.
- [39] V. Jurdjevic and H. Sussmann, *J. Diff. Equat.* **12**, 313 (1972).
- [40] T. Schulte-Herbrüggen, K. Hüper, U. Helmke, and S. J. Glaser, *Applications of Geometric Algebra in Computer Science and Engineering* (Birkhäuser, Boston, 2002), chap. Geometry of Quantum Computing by Hamiltonian Dynamics of Spin Ensembles, pp. 271–283.
- [41] F. Albertini and D. D’Alessandro, *Lin. Alg. Appl.* **350**, 213 (2002).
- [42] F. Albertini and D. D’Alessandro, *IEEE Trans. Automat. Control* **48**, 1399 (2003).
- [43] F. Mezzadri, *Notices of the Amer. Math. Soc.* **54**, 592 (2007).
- [44] T. Schulte-Herbrüggen, A. K. Spörl, K. Waldherr, T. Gradl, S. J. Glaser, and T. Huckle, in *High-Performance Computing in Science and Engineering, Garching 2007* (Springer, Berlin, to appear, 2008).
- [45] K. Waldherr, *Die Matrix-Exponentialabbildung: Eigenschaften und Algorithmen* (Diploma Thesis, Technical University Munich, 2007).
- [46] N. Khaneja, R. Brockett, and S. J. Glaser, *Phys. Rev. A* **63**, 032308 (2001).
- [47] N. Khaneja, S. J. Glaser, and R. Brockett, *Phys. Rev. A* **65**, 032301 (2002).
- [48] A. Saito, K. Kioi, Y. Akagi, N. Hashizume, and K. Ohta (2000), [quant-ph/0001113](http://arXiv.org/quant-ph/0001113).
- [49] A. Blais, *Phys. Rev. A* **64**, 022312 (2001).
- [50] R. Zeier (2007), personal communication.
- [51] M. Clausen and U. Baum, *Fast Fourier Transforms* (Bibliographisches Institut, Mannheim, 1993).
- [52] S. Egner, *Zur algorithmischen Zerlegungstheorie linearer Transformationen mit Symmetrie* (PhD Thesis, University of Karlsruhe, 1997).
- [53] A. Barenco, C. H. Bennett, R. Cleve, D. P. DiVincenzo, N. Margolus, P. W. Shor, T. Sleator, J. A. Smolin, and H. Weinfurter, *Phys. Rev. A* **52**, 3457 (1995).

APPENDIX SECTION

A. Variant-II of Scalably Assembling a Quantum Fourier Transform

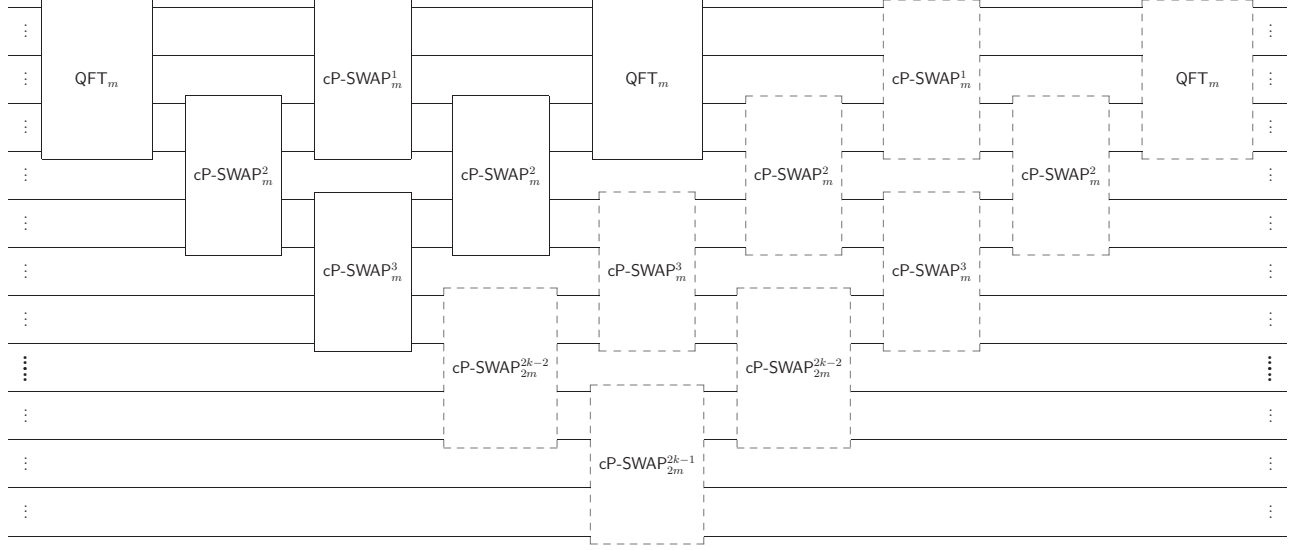


Figure 11: For $k \geq 2$ and even m , a (km) -qubit QFT can be assembled from k times an m -qubit QFT and $4\binom{k}{2}$ instances of m -qubit modules cP-SWAP_m^j , where the index j of different phase-rotation angles takes the values $j = 1, 2, \dots, 2k - 1$. The dashed boxes correspond to Fig. 6 and show the induction $k \mapsto k + 1$.

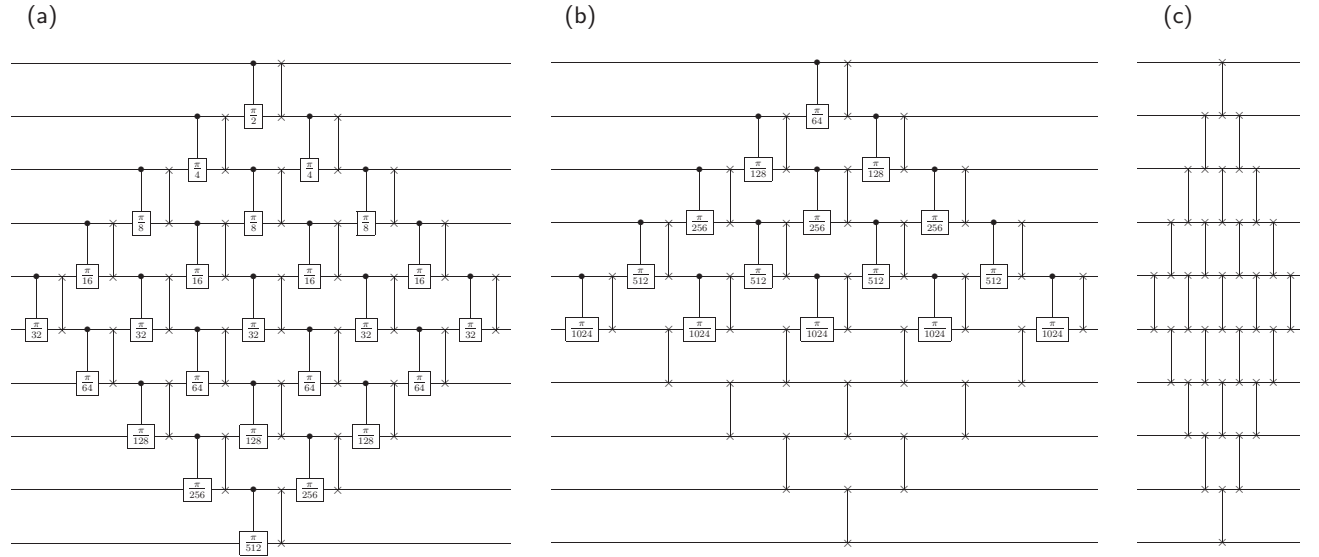
B. Controlled-Phase-SWAP Modules for $k \cdot 10$ -Qubit QFTs

Figure 12: Equivalent circuit representations of the three 10-qubit cP-SWAP modules needed for a $k \cdot 10$ -qubit QFT, when rotation angles less than $\pi/2^{10}$ are omitted (as described in the text): (a) cP-SWAP_{10}^1 with no truncation so $F_{tr} = 1$, (b) cP-SWAP_{10}^2 with $F_{tr} = 0.9999902$, and (c) cP-SWAP_{10}^j , which covers all $j \geq 3$ with fidelity $F_{tr} \geq 0.9999991$. These building blocks are compiled directly as effective 10-qubit modules thus reducing the time to less than 60% of the duration required for the decomposition into 2-qubit modules.